Materials Letters 398 (2025) 138930

Contents lists available at ScienceDirect

Materials Letters

journal homepage: www.elsevier.com/locate/matlet

Microstructure and mechanical properties of P21 tool steel fabricated via laser powder bed fusion

A. Rajesh Kannan [a,*], V. Rajkumar [b], S. Maheshwaran [c], N. Siva Shanmugam [c], Wonjoo Lee [a], Jonghun Yoon [a,*]

[a] Department of Mechanical Engineering, BK21 FOUR ERICA-ACE Center, Hanyang University, 55, Hanyangdaehak-ro, Ansan 15588 Gyeonggi-do, Republic of Korea
[b] Department of Mechanical Engineering, PSG Institute of Technology and Applied Research, Coimbatore 641062 Tamil Nadu, India
[c] Department of Mechanical Engineering, National Institute of Technology, Tiruchirappalli 620015 Tamil Nadu, India

ARTICLE INFO

Keywords:
P21 steel
Additive manufacturing
Laser powder bed fusion
Microstructure
Mechanical properties

ABSTRACT

This study examines the microstructural evolution and mechanical properties of P21 tool steel fabricated via laser powder bed fusion (LPBF). A fine martensitic matrix with minimal retained austenite forms near the top due to rapid solidification, transitioning to columnar prior austenite grains with aligned martensitic laths mid-build. Toward the bottom, microstructures coarsen, showing lath thickening and signs of tempering from thermal accumulation and cyclic reheating. These variations significantly impact mechanical behavior. P21 specimens exhibited average ultimate tensile strengths of 902 ± 20 MPa and 843 ± 5 MPa, with elongations of 23.50 ± 1.00 % and 24.70 ± 1.30 %, in the horizontal and vertical orientations, respectively. The results highlight critical structure-property relationships in LPBF-processed P21 steel and offer insights for optimizing performance in tooling applications.

1. Introduction

P21 steel is a hot work tool steel as specified in ASTM A681-24 standard, known for its excellent toughness, wear resistance, and strength [1]. P21 steel is used to produce plastic injection molds, particularly in applications demanding high precision and extended manufacturing cycles [2]. Its excellent machinability makes it ideal for complex mold designs. However, molds face wear, corrosion, and fatigue during injection molding, and replacing damaged ones increases production costs. Integrating additive manufacturing (AM) to produce P21 molds offers significant advantages over conventional methods. AM processes, such as laser powder bed fusion (LPBF), offer enhanced design flexibility and a smaller molten pool, enabling the fabrication of complex geometries [3,4]. Additionally, AM promotes efficient material usage by building components layer-by-layer, thereby minimizing waste, a crucial factor when working with high-cost tool steels like P21 [5]. Furthermore, AM can repair and refurbish worn or damaged mold components, extend tool life, and lower overall maintenance costs [6]. Recently, extensive research efforts have been devoted to developing AM-processed components that exhibit strength and ductility comparable to those produced by conventional manufacturing methods [7,8]. Fig. 1.Fig. 2..

Kim et al. [9] fabricated a multi-layered material (MLM) comprising austenitic stainless steel 316L and ferritic steel P21 using the direct energy deposition (DED) process. The P21 specimens from the MLM exhibited a tensile strength of 1050 MPa and ductility of 19.1 %. The higher strength and lower ductility are attributed to the dominant α' martensitic microstructure with minimum retained austenite, resulting from rapid cooling under a steep thermal gradient.

The AM processed P21 specimens' microstructure consists of austenite, ferrite, and martensite phases along the building direction (BD). As the build height increases, hardness decreases, primarily due to tempering effects and grain coarsening resulting from changes in thermal history and solidification rates [10]. Yu et al. [11] repaired the damaged gray cast iron-FC300 part using the additive metal-layer deposition (AMD) technology and examined the mechanical properties. The specimens repaired by the AMD process had a strength about 9 % lower than FC300. Yun et al. [12] examined the hardness and tensile properties of repaired P21 steel produced via laser-based DED process on SKD61 base material (BM). Bainite and martensite were noticed in the repaired region, and the lath martensite increased the hardness due to a higher carbon fraction. To date, the fabrication of P21 steel using AM

* Corresponding authors.
E-mail addresses: rajeshkannan@hanyang.ac.kr (A. Rajesh Kannan), yooncsmd@gmail.com (J. Yoon).

https://doi.org/10.1016/j.matlet.2025.138930
Received 10 May 2025; Received in revised form 11 June 2025; Accepted 12 June 2025
Available online 13 June 2025
0167-577X/

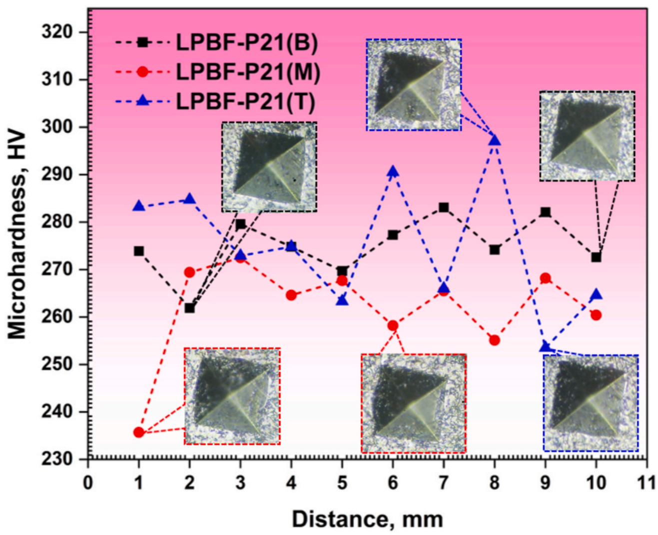

Fig. 3. Microhardness profiles along the BD at different regions.

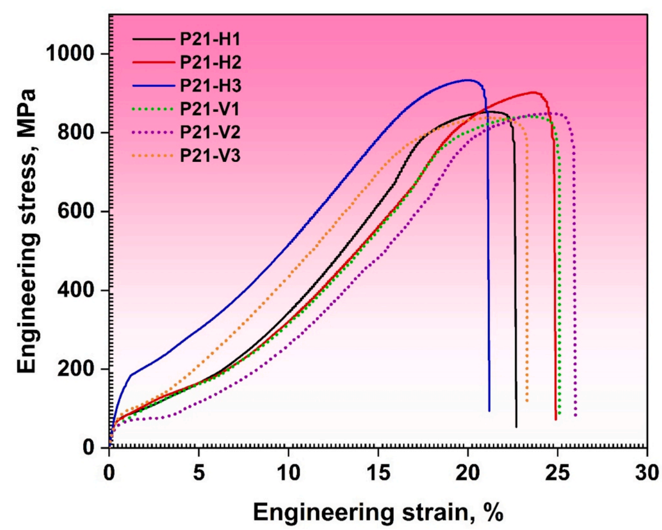

Fig. 4. Engineering stress–strain curves of LPBF-processed P21-H and P21-V specimens.

specimens, horizontal (P21-H) and vertical (P21-V) directions, reveal clear anisotropy (refer to Fig. 4). Overall, P21-H specimens exhibited higher tensile strength and similar elongation compared to P21-V ones. The average ultimate tensile strength (UTS) and ductility (EL) of P21 specimens in horizontal and vertical directions were 902 ± 20 MPa & 23.50 ± 1 % and 843 ± 5 MPa & 24.70 ± 1.30 %, respectively. Horizontal and vertical specimens showed similar plastic deformation before failure, while P21-V exhibited slightly lower UTS and higher ductility. Earlier necking and fracture in P21-V suggest microstructural differences along the loading direction relative to the BD, linked to LPBF's layer-by-layer architecture and interlayer defects. Rapid solidification in LPBF forms columnar grains aligned with the BD; P21-H specimens, loaded transverse to these grains, show higher strength, whereas P21-V specimens, loaded parallel, allow easier dislocation motion and grain boundary sliding, enhancing ductility but reducing strength.

4. Conclusion

This study investigated the microstructure and mechanical properties of P21 tool steel fabricated by LPBF process. The LPBF-fabricated P21 steel exhibits a distinct microstructural gradient along the BD. Fine martensitic structures with minimal retained austenite form at the top, while coarsened laths and tempered martensite dominate the bottom region. In addition, EDS line scan confirmed the traces of carbides in the P21 wall. The bottom region shows higher and more consistent hardness (275 ± 6 HV) due to tempered martensitic features, while the middle (262 ± 10 HV) and top (275 ± 14 HV) layers exhibit slightly lower or more variable hardness from differing thermal histories. Tensile tests reveal anisotropic behavior, with higher UTS in the horizontal (902 ± 20 MPa & 23.50 ± 1 %) direction but slightly higher ductility in the vertical (843 ± 5 MPa & 24.70 ± 1.30 %) direction. Future work should optimize heat treatment and process parameters to reduce anisotropy, improve surface hardness, and enhance stability and wear resistance for mold applications.

CRediT authorship contribution statement

A. Rajesh Kannan: Writing – original draft, Validation, Investigation, Formal analysis, Data curation. **V. Rajkumar:** Formal analysis, Data curation. **S. Maheshwaran:** Validation, Investigation, Formal analysis. **N. Siva Shanmugam:** Writing – review & editing, Resources, Methodology, Conceptualization. **Wonjoo Lee:** Validation, Investigation. **Jonghun Yoon:** Writing – review & editing, Supervision, Resources, Methodology, Funding acquisition.

Declaration of competing interest

The authors declare that they have no known competing financial interests or personal relationships that could have appeared to influence the work reported in this paper.

Acknowledgment

This work was supported by the National Research Foundation of Korea (NRF) grant funded by the Korea government (MSIT) (RS-2025-00555072). This research was financially supported by the Ministry of Trade, Industry, and Energy (MOTIE), Korea, under the "170k closed section roll forming and free curvature bending technology development for electric vehicle body" (reference number 20022814) supervised by the Korea Institute for Advancement of Technology (KIAT). This research was financially supported by MOTIE, Korea, under the "Innovative Digital Manufacturing Platform" (reference number P00223311) supervised by KIAT.

Data availability

Data will be made available on request.

References

[1] W.-S. Shin, et al., Metals (Basel) 10 (2020) 1487, https://doi.org/10.3390/met10111487.
[2] C.T. Kwok, et al., Mater. Sci. Eng. A 357 (2003) 94–103, https://doi.org/10.1016/S0921-5093(03)00228-4.
[3] J.P. Oliveira, A.D. LaLonde, J. Ma, Mater. Des. 193 (2020) 108762, https://doi.org/10.1016/j.matdes.2020.108762.
[4] X. Xi, et al., Compos. B Eng. 291 (2025) 112038, https://doi.org/10.1016/J.COMPOSITESB.2024.112038.
[5] L. Wu, et al., Adv. Eng. Mater. 23 (2021) 2100049, https://doi.org/10.1002/adem.202100049.
[6] A.R. Kannan, et al., Mater. Lett. 308 (2022) 131262, https://doi.org/10.1016/j.matlet.2021.131262.
[7] M. Liu, et al., J. Mater. Sci. Technol. 225 (2025) 111–124, https://doi.org/10.1016/j.jmst.2024.10.051.
[8] D. Lin, et al., Int. J. Plast 183 (2024) 104142, https://doi.org/10.1016/J.IJPLAS.2024.104142.
[9] D.-K. Kim, et al., J. Alloys Compd. 774 (2019) 896–907, https://doi.org/10.1016/j.jallcom.2018.09.390.
[10] M. Jo, et al., Metals (basel) 12 (2022) 2086, https://doi.org/10.3390/met12122086.
[11] J.-H. Yu, et al., Proc. Inst. Mech. Eng. B 234 (2020) 157–169, https://doi.org/10.1177/0954405419843754.
[12] B. Yun, et al., J. Korean Soc. Precis Eng. 41 (2024) 849–856, https://doi.org/10.7736/JKSPE.024.073.

[13] B.B. Straumal, et al., J. Mater. Sci. (2025), https://doi.org/10.1007/s10853-025-10854-1.
[14] B. Straumal, et al., J. Mater. Sci. (2025), https://doi.org/10.1007/s10853-025-10818-5.
[15] B. Straumal, et al., Crystals (basel) 13 (2023) 1538, https://doi.org/10.3390/cryst13111538.
[16] A.R. Kannan, et al., Mater. Lett. 274 (2020) 127968, https://doi.org/10.1016/j.matlet.2020.127968.